Proceedings of COBEM 2005
18th International Congress of Mechanical Engineering
November 6-11, 2005, Ouro Preto, MG

BIOMECHANICAL ANALYSIS OF ENDOVASCULAR ABDOMINAL AORTIC ANEURYSM REPAIR

T.V. How
School of Clinical Sciences, Division of Clinical Engineering, University of Liverpool, Liverpool, UK
e-mail thienhow@liverpool.ac.uk

S.N. Zhou
Vascular Unit, Royal Liverpool University Hospital, Liverpool, L7 8XP
e-mail s.n.zhou@liverpool.ac.uk

R. Vallabhaneni
Vascular Unit, Royal Liverpool University Hospital, Liverpool, L7 8XP
e-mail s.n.zhou@liverpool.ac.uk

Abstract. *Longitudinal haemodynamic force (LF) acting on a bifurcated stent-graft has been estimated previously using a mathematical model which assumes steady flow of an invisid fluid. An experimental method was developed, using an instrumented stent-graft model, to measure LF under human physiological and pathological blood flow conditions. The physical stent-graft model, with main trunk diameter of 30mm and limb diameters of 12mm, was fabricated from aluminium. Strain gauges were bonded onto the main trunk to determine the longitudinal strain which is related to LF. After calibration, the bifurcated was placed in a pulsatile flow system with glycerol solution as circulating fluid. Strain was determined using a Wheatstone bridge signal conditioning circuit. The signals were averaged over 600 cardiac cycles and saved to a PC for subsequent processing. LF was strongly dependent on pressure and diameter but less so on flow rate. The pulsatile flow resulted in transient force which was higher than that predicted by the simplified mathematical model, but lower at peak systole. Under certain conditions, e.g., large device diameter, hypertension and large main trunk-to-iliac limb diameter ratio, the LF may exceed the fixation force of current clinical endovascular stent-grafts.*

Keywords*: EVAR, Endoleak, Haemodynamic force, Stent-graft,*

1. Introduction

Abdominal aortic aneurysm (AAA) is a common vascular disorder which affects up to 5% of the male population over 55 years of age in the Western hemisphere. Surgical replacement of the diseased aortic segment using a bifurcated aortic fabric graft has been the standard treatment of AAA. Endovascular repair (EVAR) using an endoluminal stent-graft to exclude the AAA is an alternative that is finding wide acceptance throughout the world since it was first used clinically by Parodi *et al* (1991). Being minimally invasive, recovery of the patients is much quicker and obviates the need for cross-clamping of the aorta. The primary purpose of EVAR is to prevent death from aneurysm rupture. As with standard open repair, the aim of intervention is to isolate the aneurysm from the aortic or systemic pressure while maintaining flow to the lower limbs. The early results of EVAR show a significant improvement in 30 day mortality over conventional, which is maintained over the follow-up period of 4 years (Trial participants, 2005). Mid-term results, however, have revealed a number of complications namely endoleak, distal migration of the device, thrombosis and occlusion necessitating regular surveillance of the patients. These complications represent significant causes of surgical re-nterventions (Harris et al, 2000).

The success of EVAR depends on secure fixation of the sent-graft in the patient's aorta. The fixation strength has been estimated by measuring the longitudinal displacement force at the proximal fixation site of various commercially available stent grafts in a cadaveric model [4]. The average distraction force ranged from 4.5 N to 25 N, compared to 150 N for the hand sewn anastomosis in conventional repair.

In a previous clinical study we showed that hypertension, aneurysm geometry and iliac angulation, amongst other factors, were significantly associated with stent-graft migration [5]. These findings were validated using a simplified mathematical model based on momentum equation and neglects the pulsatility of blood flow and the viscosity of the fluid. It was shown that under certain conditions, the longitudinal force (LF) on the EVAR device due to blood flow and pressure may exceed the fixation force causing device migration. The purpose of this study is to develop an experimental method to measure LF in a model of a stent-graft under pulsatile flow of a viscous fluid. A number of test runs were carried out to assess the feasibility of the technique and compare the experimental and theoretical values.

2. Theoretical Model

We consider a simple model an idealized bifurcated device shown in Figure 1 to estimate the longitudinal force f_x exerted on the EVAR device. We assume that the bifurcation is planar and symmetrical and the blood flow is

distributed equally through two iliac limbs. Fluid entering the device splits equally into the two iliac limbs of equal diameter. The change in direction and velocity of flow due to the diameter change and the bifurcation angle causes a change in the momentum of the fluid. The momentum change and the pressure forces acting at the inlet and outlets result in a net longitudinal force f_x on the device which must be opposed to prevent its distal migration.
We have shown previously that f_x can be estimated by equation (1) [5].

$$P_1 A_1 - 2P_2 A_2 \cos\theta - f_x = \rho Q\left(\frac{U_2}{2}\cos\theta + \frac{U_2}{2}\cos\theta - U_1\right) \tag{1}$$

where P_1, A_1, U_1 and P_2, A_2, U_2 are the pressure, cross-sectional area and velocity at the inlet and outlet, respectively; ρ is the density of the fluid and Q is the volume flow rate. The first two terms on the left hand side of equation (1) represent the pressure forces at the inlet and outlets acting on areas A_1 and A_2, respectively. f_x is the axial component of the force exerted by the bifurcation on the fluid. The right hand side of equation (1) represents the rate of increase of axial component of momentum.

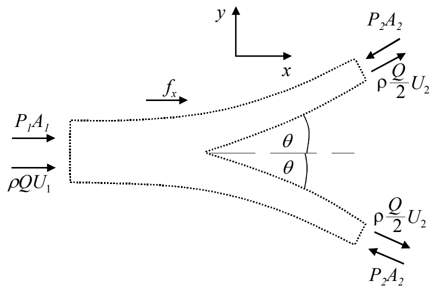

Figure 1: Geometry haemodynamic conditions and longitudinal force f_x in a bifurcated stent-graft.

Using Bernoulli's and continuity equations we can obtain an equation for f_x as follows:

$$\begin{aligned} f_x = {} & P_1 A_1 + \rho A_1 U_1^2 - \rho\frac{A_1^2}{2A_2}U_1^2\cos\theta - \\ & 2A_2\cos\theta\left[P_1 + \rho\frac{U_1^2}{2}\left(1 - \frac{A_1^2}{4A_2^2}\right)\right] \end{aligned} \tag{2}$$

f_x can be readily calculated for any device geometry and haemodynamic conditions using equation (2). In the transverse direction the pressure and momentum forces cancel out because of the symmetry and equal flow distribution and therefore $f_y = 0$.

3. Materials and Method

3.1. Measurement of Longitudinal force in an Instrumented Model of a Bifurcated EVAR Device

We consider only the main trunk portion of the graft model . Figure 2 shows that this section is subjected to a transmural pressure P and a longitudinal force F. Here F represents the net resultant force due to the pressure force at the iliac limbs, the force due to the momentum change and the viscous drag force.

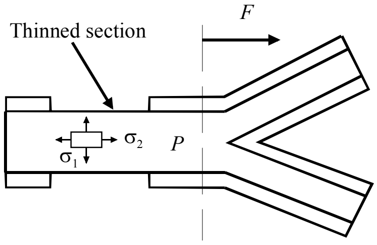

Figure 2. Longitudinal and circumferential stresses in a cylinder due to transmural pressure P and longitudinal force F. R is the radius and T is the wall thickness of the thinned segment.

The following 2-dimensional stress equations for a pressurised cylinder can be applied to the thinned section of the stent-graft model.

$$\sigma_1 = \frac{PR}{T} \qquad \text{(Circumferential stress)}$$

$$\sigma_2 = \frac{PR}{2T} \qquad \text{(Longitudinal stress)}$$

With the addition of the longitudinal force F the stresses become:

$$\sigma_1 = \frac{PR}{T} \tag{3}$$

$$\sigma_2 = \frac{PR}{2T} + \frac{F}{2\pi RT} \tag{4}$$

The graft model is instrumented by means of strain gauges bonded onto the external surfaces of the cylindrical segment. The strains in the circumferential and longitudinal directions due to these stresses can be obtained by the principle of superposition.

Circumferential strain (e_1) = strain caused by σ_1 + strain caused by σ_2

$$e_1 = \frac{\sigma_1}{E} - \frac{\nu\sigma_2}{E} = \frac{1}{E}\left[\sigma_1 - \nu\sigma_2\right] \tag{5}$$

where E is the Young's modulus and ν the Poisson's ratio of he tube material. Similarly,

$$e_2 = \frac{1}{E}\left[\sigma_2 - \nu\sigma_1\right] \tag{6}$$

Substituting:

$$\frac{PR}{2T} = \hat{P}$$

and

$$\frac{F}{2\pi RT} = \hat{F}$$

in equations (3) and (4):

$$\sigma_1 = 2\hat{P} \tag{7}$$

$$\sigma_2 = \hat{P} + \hat{F} \tag{8}$$

We now substitute eqns (7) and (8) into eqns (5) and (6)

$$e_1 = \frac{1}{E}\left[2\hat{P} - \nu(\hat{P} + \hat{F})\right] = \frac{1}{E}\left[(2-\nu)\hat{P} - \nu\hat{F}\right] \tag{9}$$

$$e_2 = \frac{1}{E}\left[(\hat{P} + \hat{F}) - 2\nu\hat{P}\right] = \frac{1}{E}\left[(1-2\nu)\hat{P} + \hat{F}\right] \tag{10}$$

We are interested in determining the total longitudinal force by measuring F as well as e_2. Equation (10) can be re-written as follows:

$$e_2 = \left[(1-2\nu)\frac{R}{2ET}P + \frac{1}{2\pi ERT}F\right] \tag{13}$$

If we can find the following terms:

$$(1-2\nu)\frac{R}{2ET}, \quad \frac{1}{2\pi ERT}, \quad \text{and} \quad P$$

Then we should be able to determine *F*. First we calibrate the sensor without pressure.

$$\sigma_1 = 0$$

$$\sigma_2 = \frac{F}{2\pi RT}$$

From eqns (3) and (4):

$$e_1 = \frac{1}{E}\left[-\frac{\nu}{2\pi RT}F\right]$$

$$e_2 = \frac{1}{E}\left[\frac{1}{2\pi RT}F\right]$$

Rewriting e_2

$$e_2(\text{volt}) = \frac{1}{2\pi RTE} \cdot F(\text{N})$$

We can therefore obtain the term $1/(2\pi RTE)$ in terms of volt/N. Next, we apply pressure only.

From eqns (3) and (4):

$$e_1 = \frac{1}{E}\left[2\hat{P} - \nu\hat{P}\right]$$

$$e_2 = \frac{1}{E}\left[\hat{P} - 2\nu\hat{P}\right]$$

Rewriting e_2:

$$e_2 = \frac{(1-2\nu)}{E}\frac{R}{2T} \cdot P$$

We can therefore determine $(1\text{-}2\nu)R/2ET$ in terms of volt/mmHg. *P* will be measured near the main trunk.

3.2. Stent-Graft Model

The model was made from machined aluminium tubes joined with metal-loaded epoxy resin to form a bifurcation. The main trunk of internal diameter 30mm and wall thickness 4 mm has a thinned segment 30 mm long and 0.1 mm wall thickness. The thinned segment was provided in order to increase the level of strains locally. Four strain gauges (CEA-13-250UN-350, Vishay Micro-Measurements, Reading, UK) from the same batch were bonded onto thinned section using cyanoacrylate, two strain gauges were orientated longitudinally and the other two, circumferentially. Each pair was connected in a half-bridge configuration and two high stability precision resistors were used to complete the Wheatstone bridge. To minimise the effect of temperature changes, the dc bridge supply voltage was set to 1.25 or 2.5 V.

After calibration, as described above, the model was placed in a pulsatile flow circuit described previously [6]. The pressure, flow and e_2 (the longitudinal force) waveforms were each sampled at 100 samples/s and saved to a PC for subsequent analysis.

4. Results

The results of a run at a mean flow rate of 1.5 l/min, mean and pulse pressures of 120 mmHg and heart rate of 60 beats/min are shown in Figures 4, 5 and 6. Each waveform was averaged over 600 cardiac cycles. The force and pressure waveform appear to be almost in phase. The peak force occurred about 40 ms later than peak pressure.

The measured LFs shown in Figure 6 were higher than those predicted by equation (2). For example, at the minimum pressure of 78.5 mmHg (430 ms) and peak pressure of 184.4 mmHg (140 ms), the measured LF was 7.8 N and 12.7 N compared to theoretical values of 6.3N and 15.0 N, respectively.

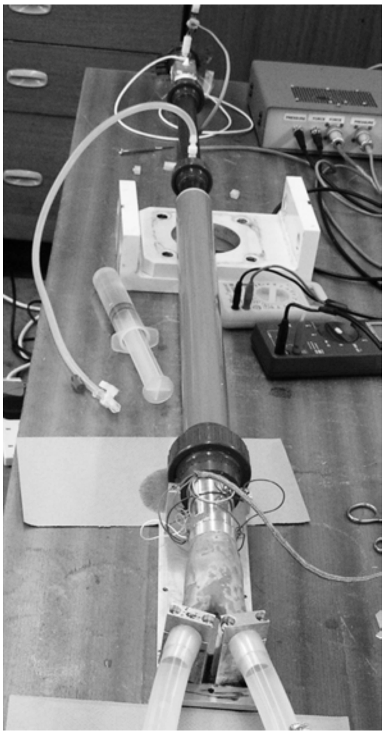

Figure 3. Bifurcated stent-graft model with strain gauges atttached and inlet and outlet pipes.

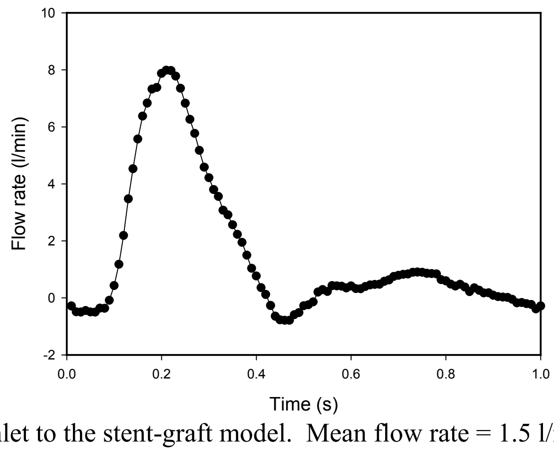

Figure 4: Flow waveform inlet to the stent-graft model. Mean flow rate = 1.5 l/min., Heart rate = 60 beats/min.

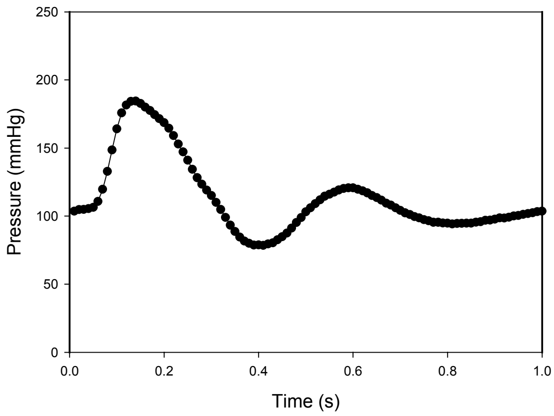

Figure 5: Pressure waveform simulating hypertension. The mean pressure = 113 mmHg, minimum pressure = 78.5 mmHg, peak pressure = 184 mmHg.

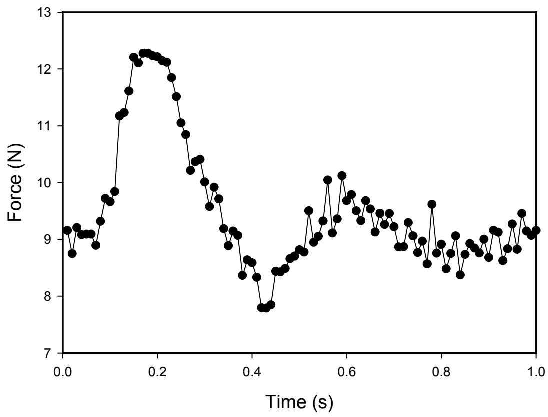

Figure 6: Variation in measured LF during the flow cycle.

4. Discussion

Equation (2) was derived using a number of simplifying assumptions about the fluid and the geometry of the bifurcation. These initial results show that the measured LFs are similar to those predicted by the simplified model. In diastole, LF is underestimated while at peak systole it is overestimated by the simplified model. The difference may be due to the effect of viscosity and the pulsatility of flow. We are carrying out further studies with fluids of different viscosity and different flow and pressure waveforms to assess the influence of these two parameters.

These results confirm that under certain conditions, LF can exceed the fixation force of some of the current endovascular stent-grafts and may therefore lead to the distal migration and rupture of the aneurysm

5. References

Chong, C.K., How T.V., 2004, “Flow patterns in an endovascular stent-graft for abdominal aortic aneurysm repair”, Journal of Biomechanics, Vol.37, pp. 89-97.

Evar Trial Participants, 2005, “Endovascular aneurysm repair versus open repair in patients with abdominal aortic aneurysm (EVAR trial 1): randomised controlled trial”, Lancet, Vol.365, pp. 2179-86.

Harris, P.L., Vallabheneni S.R., Desgranges P., Becquemin J.P., Van Marriewijk C., Laheij R.J., 2000 “Incidence and risk factors of late rupture, conversion, and death after endovascular repair of infrarenal aortic aneurysms: the EUROSTAR experience”, Journal of Vascular Surgery, Vol.32, pp. 739-49.

Mohan, I.V., Harris, P.L., Van Marriewijk, C., Laheij, R.J.F. How, T.V., 2002, “Factors and forces influencing stent-graft migration after endovascular aortic aneurysm repair”, Journal of Endovascular Therapy, Vol.9, pp. 748-755.

Parodi, J. C., Palmaz, J. C., Barone, H. D., 1991, “Transfemoral intraluminal graft implantation for abdominal aortic aneurysms” Annals of Vascular Surgery, Vol.5, pp.491-499.

Resch, T., Ivancev, K., Brunkwall, J., Nyman, U., Malina, M., Lindblad, B., 1999 “Distal migration of stent-grafts after endovascular repair of abdominal aortic aneurysms”, Journal of Vascular Interventional Radiology, Vol.10, pp. 257-264.